A FINITE ELEMENT ANALYSIS OF A CIRCUMFERENTIALLY NOTCHED TENSILE SPECIMEN

D. K. Brown* and R. M. McMeeking**

INTRODUCTION

Over the past few years much research has been carried out at the University of Glasgow into ductile fracture. Much of the experimental work has involved the use of circumferentially notched tensile specimens [1]. By varying the ratio of minimum cross-section radius a_o to notch radius R, Figure 1, the constraint in the centre of the specimen can be varied. A series of tests on different materials using five different specimen geometries allowed failure curves to be drawn. The initial ratios (a_o/R) varied from 1 (A-notch) to 3 (D-notch). Forming the axes of such graphs are the parameters mean to effective stress ratio, $\sigma_m/\bar{\sigma}$, and strain to failure, $\bar{\varepsilon}_f$, both evaluated at the centre of the bar. In terms of principal stresses, $\sigma_m = (\sigma_1 + \sigma_2 + \sigma_3)/3$, $\bar{\sigma} = [(\sigma_1 - \sigma_2)^2 + (\sigma_2 - \sigma_3)^2 + (\sigma_3 - \sigma_1)^2]^{1/2}$ and $\bar{\varepsilon}_f$ is defined in [1] as the average value of effective plastic strain across the minimum section at failure initiation, which is detected by a significant drop in load bearing capacity. Combining the failure curves with a material size parameter and the approximate expression [2], $\delta = 0.6K_I^2/E\sigma_y$ enabled prediction of C.O.D. and critical defect size. These latter parameters were determined using small scale circumferentially notched specimens, with obvious economic advantages.

In determining the stress ratio and strain from the tests use was made of the work of Bridgman [3], which dealt with naturally necking bars. Confirmation of the accuracy of applying Bridgman's analysis to pre-notched bars is obviously advisable and two approaches were made. The first approach [4] was experimental and involved the analysis of deformation in the mid-section of banded steel specimens. Three geometries were analysed, the results indicating much better agreement with Bridgman for the A-notch than for the D-notch. Comparison was also made to the results of Clausing [5] who also used banded specimens of different geometry. Clausing compared his results with a modified form of the Bridgman analysis.

The results from the second approach are presented below, they being derived from a finite element solution of the A-notch. A finite element solution was also used by Argon, Im and Needleman [6], but this was for a naturally necking bar.

PROGRAMME

The results were generated using an early version of the MARC finite element programme which was subsequently modified by Rice and Tracey [7]. The programme has a finite strain capability [8] and uses an incremental determination of the solution [7]. The elements used were isoparametric quadrilaterals over which uniform dilation was enforced [9].

*University of Glasgow, Scotland.
**Brown University, Providence, R.I., U.S.A.

Only a symmetrical quarter of the specimen cross-section need be considered and the finite element grid, Figure 1, was chosen to concentrate elements in areas of high stress and strain gradients. The shape of the elements on or near the section BC was chosen such that even after large deformations, element aspect ratios were kept to a minimum. The power law stress-strain curve used, can be defined by

$$\left(\frac{\bar{\sigma}}{\sigma_y}\right)^{1/n} - \frac{\bar{\sigma}}{\sigma_y} = \frac{3G\bar{\varepsilon}^p}{\sigma_y} \quad \text{for } \frac{\bar{\sigma}}{\sigma_y} \geq 1$$

where σ_y is the uniaxial yield stress. Two values of index n = 0.1, 0.2 were selected and the elastic perfectly plastic case was also solved. The grid was 'loaded' by application of uniform displacement along boundary AE, the displacement to cause initial yielding at C being denoted by 100%. 24 graded increments of uniform displacement produced a final 'load' of 990%.

RESULTS

The results presented here are for the case of n = 0.2 power hardening, this material response being closest to the ENIA low carbon steel used in the experiments of Earl and Brown [4]. Comparison is made between these latter results, the computer results, and the Bridgman approximation, based on the specimen shapes and computed by finite elements.

(1) *Profiles and Plastic Zone shapes.* Figure 2 illustrates the profile of the A notch, when elastic, and after deformation of 990%. In order to calculate the current radius of curvature, R, of the notch at C (Figure 1) the displacements of point 1, 2, 3 were considered. With the reduced cross-section radius, a, the ratio (a/R) can be determined and three values are shown on Figure 2. The initial value of ratio is 1.0 and, as plasticity develops, the value drops to 0.932 at 310% before returning to 1.0 when a significant proportion of the notch is flowing plastically. The increasing plastic zone is illustrated in Figure 3.

As the power hardening index drops there is a noticeable drop in plastic zone size, at the same boundary displacement of 990% but with a corresponding increase in plastic strain and deformation on the mid-section BC. The ratios (a/R) at 990% for n = 0.1 and the perfectly plastic case are 1.14 and 1.29 respectively.

(2) *Radial Displacement* U *on* BC. It is of interest to plot the ratio U/U_c (where U_c is the radial displacement of C) against radius across BC. Bridgman assumes a straight line and, as can be seen from Figure 4, the trend from the elastic to the plastic (990%) distribution is towards this straight line.

(3) *Distribution of Effective Plastic Strain.* Figure 5 shows the distribution of effective plastic strain $\bar{\varepsilon}^p$ along the boundaries ABCD (Figure 1) for 990% where $\bar{\varepsilon}^p$ can be defined, in principal strains, as

$$\bar{\varepsilon}^p = \int \left[\left(d\varepsilon_1^p - d\varepsilon_2^p\right)^2 + \left(d\varepsilon_2^p - d\varepsilon_3^p\right)^2 + \left(d\varepsilon_3^p - d\varepsilon_1^p\right)^2\right]^{1/2}$$

Across the neck Bridgman assumed a uniform value of effective plastic strain, this best being considered an average value, which is given by

$$\bar{\varepsilon}^p_{ave} = 2 \ln\left(\frac{a_o}{a}\right)$$

At 990%, $\bar{\varepsilon}^p_{ave}$ is 21.1% and this value is shown on Figure 5. Values of $\bar{\varepsilon}^p_{ave}$ for n = 0.1 and the perfectly plastic case are 26.1% and 30.7% respectively for 990%, reflecting equally well the higher mean values of the $\bar{\varepsilon}^p$ distribution for the corresponding finite element solutions. As power hardening drops the peak value of $\bar{\varepsilon}^p$ moves from C to B. In Earl and Brown [4] the A4 specimen has $\bar{\varepsilon}^p_{ave} = 27.7\%$ and cannot be compared exactly but the trend of $\bar{\varepsilon}^p$ is similar to Figure 5.

(4) *Stresses* $\sigma_r\ \sigma_\theta\ \sigma_z$. On Figure 6 are plotted the normal stress distributions down ℄ AB and across the mid-section BC, for both the elastic (100%) and plastic (990%) conditions. From equilibrium, σ_r and σ_θ are always equal along AB and σ_r always drops to zero at C. However on BC at 990% σ_r, σ_θ follow almost a common curve down to zero at C a trend predicted by Bridgman. Quantitatively, however, for the A-notch, the distributions are not as accurate. They are calculated using assumed stress flow lines, from

$$\sigma_r = \sigma_\theta = \bar{\sigma} \ln\left[\frac{1}{2}\left(\frac{a}{R}\right)\left(1 - \left(\frac{r}{a}\right)^2\right) + 1\right]$$

Using the (a/R) ratio from Figure 2 the Bridgman approximation is drawn on Figure 5. Similarly the curve for σ_z is calculated from

$$\sigma_z = \bar{\sigma}\left\{1 + \ln\left[\frac{1}{2}\left(\frac{a}{R}\right)\left(1 - \left(\frac{r}{a}\right)^2\right) + 1\right]\right\}$$

The value for $\bar{\sigma}$ used above comes from the stress/strain curve at the value corresponding to $\bar{\varepsilon}^p_{ave}$.

At 990%, as the power hardening drops to the perfectly plastic case, the peak value of σ_r/σ_y, σ_θ/σ_y at B vary very little although the Bridgman value drops to 0.5. However the peak values of σ_z/σ_y drop to around 2.25 and the Bridgman values to around 1.5. Comparison with the Earl and Brown A4 specimen at $\bar{\varepsilon}^p_{ave} = 27.7\%$ indicates peak values of σ_z/σ_y and σ_θ/σ_y, σ_r/σ_y at B of 2.2 and 0.5 respectively, the differences reflecting the experimental difficulty of determining mean stress.

(5) *Distribution of* $\sigma_m/\bar{\sigma}$. The distributions of this stress ratio, which indicates the severity of stress state are shown on Figure 7 for the elastic (100%) and plastic (990%) conditions. Little variation is detected with load and a favourable comparison can be made with the Bridgman approximation, which is calculated from

$$\frac{\sigma_m}{\bar{\sigma}} = \frac{1}{3} + \ln\left[\frac{1}{2}\left(\frac{a}{R}\right) + 1 - \frac{(r/R)^2}{2(a/R)}\right]$$

At 990% and lower work-hardening the Bridgman curves vary very little while the finite element solutions show the peak at B rising to over 1.5.

CONCLUSIONS

The results quoted are perforce a short summary of all the results generated and it is hoped in the near future to publish a more comprehensive comparison of the results of several notch shapes, such as the D-notch [1] and the notch used by Clausing [5]. From the comparisons made herein, it can be seen that the approximate Bridgman results are remarkably good for this pre-notched geometry and bear witness to his remarkable insight.

ACKNOWLEDGEMENTS

Thanks are due to the University of Rhode Island, Kingston, R.I., U.S.A. where the initial results were generated and to the University of Glasgow, Scotland where the final runs were completed. One of us (RMM) was supported by the U.S. Energy Research and Development Admiministration. Gratitude is expressed to Professor J. R. Rice of Brown University, Providence, R.I. for many helpful discussions.

REFERENCES

1. MACKENZIE, A. C., HANCOCK, J. W. and BROWN, D. K., To be published in Engng. Frac. Mechs.
2. RICE, J. R. and JOHNSON, M. A., "Inelastic Behaviour of Solids", (M. F. Kanninen et al. Eds.), McGraw Hill, 1970, 641.
3. BRIDGMAN, P. W., "Studies in Large Plastic Flow and Fracture", McGraw Hill, 1952.
4. EARL, J. C. and BROWN, D. K., To be published in Engng. Frac. Mechs.
5. CLAUSING, D. P., J. Materials, 4, 1969, 566.
6. ARGON, A. S., IM, J. and NEEDLEMAN, A., Met. Trans, 6A, 1975, 815.
7. RICE, J. R. and TRACEY, D. M., "Numerical and Computer Methods in Structural Mechanics", (S. J. Fenves et al. Eds.), Academic Press, 1973.
8. McMEEKING, R. M. and RICE, J. R., Int. J. Solids, Struc. 11, 1975, 601.
9. NAGTEGAAL, J. C., PARKS, D. M. and RICE, J. R., Comp. Meth. in Appl. Mech. and Engng., 4, 1974, 153.

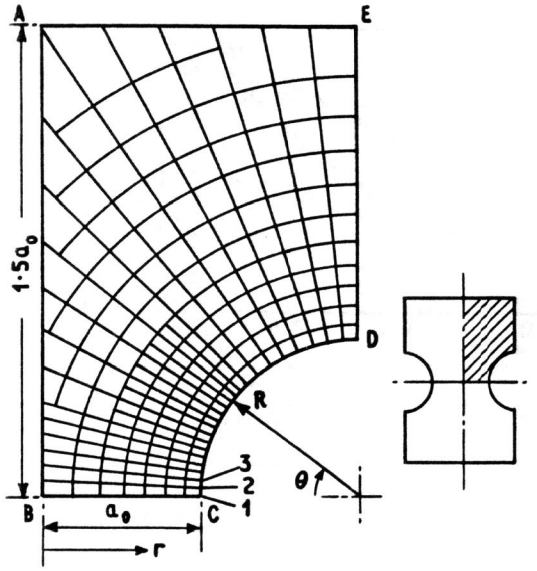

Figure 1

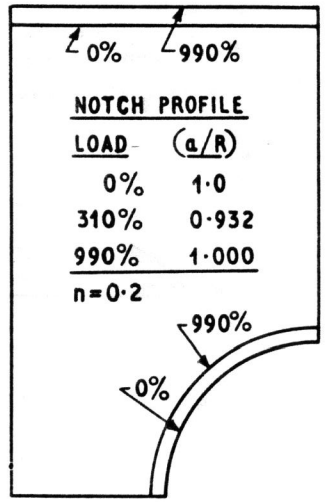

Figure 2

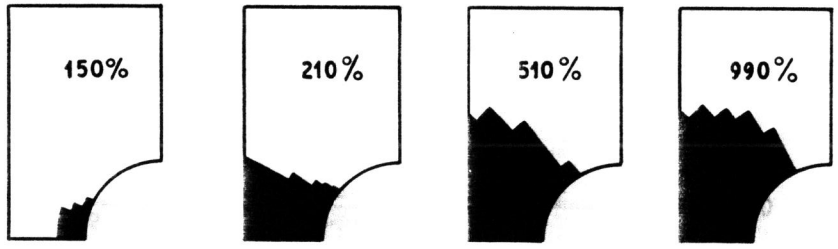

Figure 3 Development of Plastic Zone n = 0.2

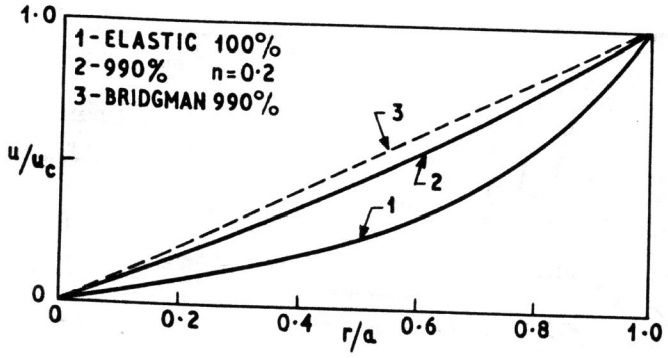

Figure 4 Radial Displacement at Neck

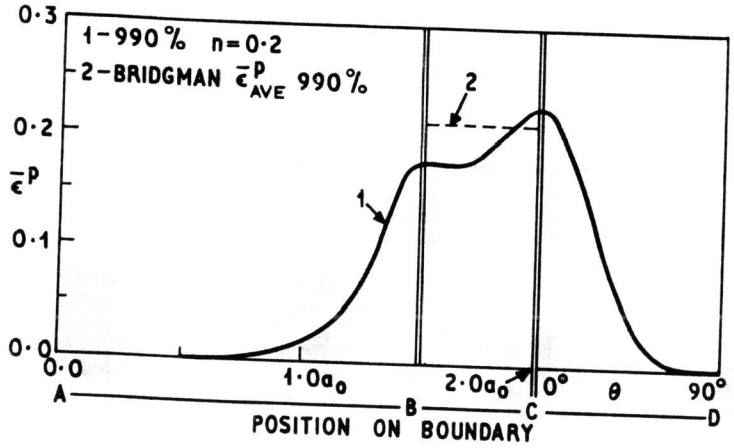

Figure 5 Distribution of Effective Plastic Strain

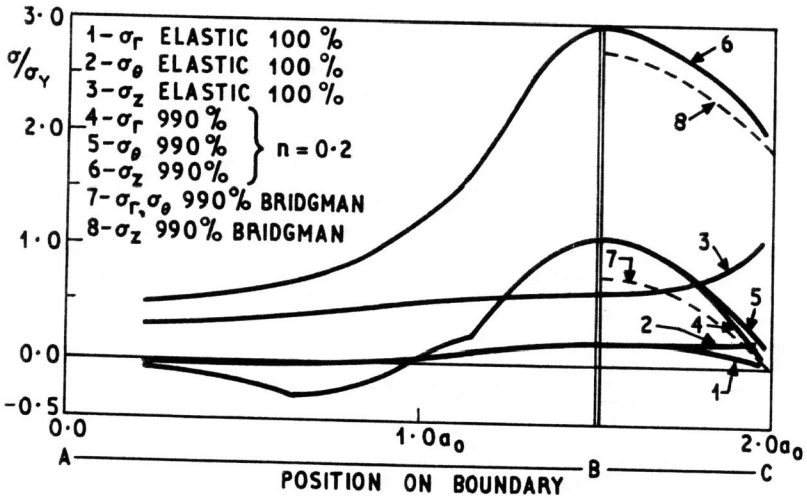

Figure 6 Stress Distributions

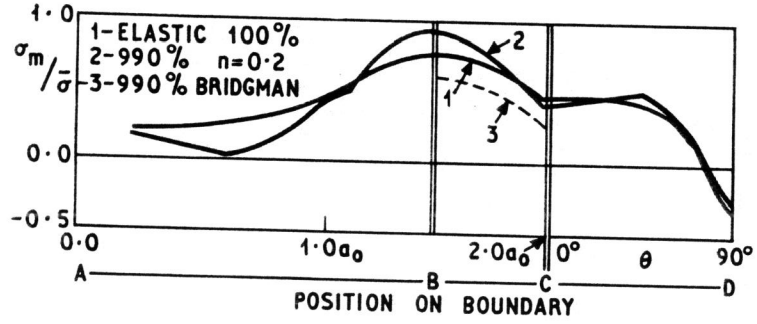

Figure 7 Distributions of $\sigma_m/\bar{\sigma}$